ELSEVIER

International Journal of Refrigeration 23 (2000) 43–63

REVUE INTERNATIONALE DU FROID
INTERNATIONAL JOURNAL OF
refrigeration

www.elsevier.com/locate/ijrefrig

An extended corresponding states model for the thermal conductivity of refrigerants and refrigerant mixtures☆

Mark O. McLinden*, Sanford A. Klein[1], Richard A. Perkins

Physical and Chemical Properties Division, National Institute of Standards and Technology, Boulder, CO 80303 USA

Accepted 1 April 1999

Abstract

The extended corresponding states (ECS) model of Huber et al. (Huber, M.L., Friend, D.G., Ely, J.F. Prediction of the thermal conductivity of refrigerants and refrigerant mixtures. Fluid Phase Equilibria 1992;80:249–61) for calculating the thermal conductivity of a pure fluid or fluid mixture is modified by the introduction of a thermal conductivity shape factor which is determined from experimental data. An additional empirical correction to the traditional Eucken correlation for the dilute-gas conductivity was necessary, especially for highly polar fluids. For pure fluids, these additional factors result in significantly improved agreement between the ECS predictions and experimental data. A further modification for mixtures eliminates discontinuities at the pure component limits. The method has been applied to 11 halocarbon refrigerants, propane, ammonia, and carbon dioxide as well as mixtures of these fluids. The average absolute deviations between the calculated and experimental values ranged from 1.08 to 5.57% for the 14 pure fluids studied. Deviations for the 12 mixtures studied ranged from 2.98 to 9.40%. Deviations increase near the critical point, especially for mixtures. Published by Elsevier Science Ltd.

Keywords: Refrigerant; Mixture; Physical property; Thermal conductivity; Model; Calculation; Corresponding states

Modèle d'états correspondants étendus pour la conductivité thermique de frigorigènes et de mélanges de frigorigènes

Resumé

Le modèle d'états correspondants étendus (ECS) de Huber et al. (Huber, M.L., Friend, D.G., Ely, J.F. Prediction of the thermal conductivity of refrigerants and refrigerant mixtures. Fluid Phase Equilibria 1992 ;80 :249-61) permettant le calcul de la conductivité thermique d'un frigorigène pur ou d'un mélange de frigorigènes est ici modifié par l'introduction d'un facteur de forme de la conductivité thermique qu'on détermine à partir des données expérimentales. Il a fallu applique une correction empirique supplémentaire (en plus de la corrélation d'Eucken en général utilisée pour la conductivité des gaz dilués), surtout pour des frigorigènes fortement polaires. Pour les frigorigènes purs, ces facteurs supplémentaires ont donné lieu a une plus grande concordance entre les prévisions ECS et les données expérimentales. Une modification de plus élimine les discontinuités limites des composants purs. On a appliqué cette méthode à 11 frigorigènes hydrocarbures

☆ Contribution of the National Institute of Standards and Technology, not subject to copyright in the United States.

* Corresponding author. Tel.: +1-303-497-3580; fax: +1-303-497-5224.

E-mail address: markm@boulder.nist.gov (M.O. McLinden)

[1] Permanent address: Solar Energy Laboratory, University of Wisconsin, Madison, WI, 53706, USA.

0140-7007/00/$20.00 Published by Elsevier Science Ltd.
PII: S0140-7007(99)00024-9

halogénés, à propane, à l'ammoniac et au dioxyde de carbone ainsi qu'à des mélanges de ces frigorigènes. Les déviations moyennes entre les valeurs calculées et expérimentales variaient de 1,08 à 5,57 % pour les 14 frigorigènes purs étudiés. Les déviations augmentent aux alentours du point critique, surtout pour les mélanges. Published by Elsevier Science Ltd.

Mots clés: Frigorigène ; Mélange ; Propriété physique ; Conductivité thermique ; Calcul ; Etat correspondant

Nomenclature

A	molar Helmholtz energy
AAD	average absolute deviation, defined in Eq. (23)
C	constant in Eq. (13)
C_P^*	ideal-gas heat capacity at constant pressure
f	equivalent substance reducing ratio for temperature
f_{int}	factor in Eucken correlation for dilute-gas contribution
F_λ	multiplier for thermal conductivity, defined in Eq. (17)
h	equivalent substance reducing ratio for density
M	molar mass
P	pressure
R	molar gas constant
T	absolute temperature
x	composition (mole fraction)
X	objective function for minimization defined in Eq. (18)
Z	compressibility factor
α	reduced molar Helmholtz energy
χ	thermal conductivity shape factor
λ	thermal conductivity
ε/k	molecular energy parameter
ϕ_{ji}	function in Wassiljewa equation, defined in Eq. (25)
ϕ	shape factor for density
η^*	dilute-gas viscosity
ρ	molar density
σ	molecular size parameter
θ	shape factor for temperature
$\Omega^{(2,2)}$	collision integral

Subscripts

i, j	fluid of interest
ij	binary pair of interest
mix, x	mixture quantity
r	reduced quantity
0	reference fluid

Superscripts

c.e.	critical enhancement
crit	critical point
int	thermal conductivity arising from internal motions

1. Introduction

We present a model for the thermal conductivity of refrigerants based on the extended corresponding states (ECS) concept. The principle of corresponding states stems from the observation that the properties of many fluids are similar when scaled by their respective critical temperature and density. The extended corresponding states models modify this scaling by additional "shape factors" to improve the representation of data. ECS methods have often been used to represent both the thermodynamic and transport properties of a fluid, especially fluids with limited data. Recently, high-accuracy equations of state have been developed for many of the refrigerants of industrial interest. But the situation for the transport properties of viscosity and thermal conductivity lags the thermodynamic properties — accurate, wide-ranging, fluid-specific correlations are available for only a few refrigerants. There is a need for a method which can predict the transport properties in the absence of data yet also take advantage of whatever experimental data might be available to improve upon the purely predictive scheme.

The method we present starts with the ECS model of Huber et al. [1]. We combine this predictive model with the best available thermodynamic equations of state. Furthermore, when thermal conductivity data are available, we use those data to fit a new "thermal conductivity shape factor" and/or a term in the traditional correlation for the dilute-gas portion of the thermal conductivity. This new modification is analogous to our earlier work on viscosity [2].

2. Pure-fluid thermal conductivity

We follow the formalism of Ely and Hanley [3] and Huber et al. [1], which represents the thermal

conductivity of a fluid as the sum of two parts — energy transfer due to translational and internal contributions

$$\lambda(T,\rho) = \lambda^{\text{trans}}(T,\rho) + \lambda^{\text{int}}(T), \tag{1}$$

where the superscript "trans" designates the translation term, i.e. contributions arising from collisions between molecules, and the superscript "int" designates the contribution from internal motions of the molecule. The internal term is assumed to be independent of density. The translation term is divided into a dilute-gas contribution λ^* and a density-dependent term, which is further divided into a residual part (superscript r) and a critical enhancement (superscript crit). The thermal conductivity is thus the sum of four terms:

$$\lambda(T,\rho) = \lambda^{\text{int}}(T) + \lambda^*(T) + \lambda^{\text{r}}(T,\rho) + \lambda^{\text{crit}}(T,\rho) \tag{2}$$

This paper focuses on the residual term, which is the dominant contribution to the thermal conductivity of liquids and dense fluids away from the critical region. We adopt the standard formulas for the dilute-gas contributions which arise from kinetic theory and which have been used by Ely and Hanley [3], Huber et al. [1], and others, but with an empirical modification. We use an empirical approach to the critical enhancement. Each of these contributions is discussed in turn.

2.1. Dilute-gas contribution

The transfer of energy associated with internal degrees of freedom of the molecule is assumed to be independent of density and can be calculated using the Eucken correlation for polyatomic gases [4]:

$$\lambda_j^{\text{int}}(T) = \frac{f_{\text{int}}\eta_j^*(T)}{M_j}\left[C_{P,j}^* - \frac{5}{2}R\right], \tag{3}$$

where C_P^* is the ideal-gas heat capacity, R is the gas constant, M is the molar mass, and η^* is the dilute gas viscosity. The subscript j emphasizes that all quantities are to be evaluated for fluid j.

The factor f_{int} in Eq. (3) accounts for the energy conversion between internal and translational modes. It is a constant equal to 1×10^{-3} in the original Eucken correlation when R and C_P^* are in J/(mol K), η^* is in μPa s, M is in g/mol, and λ is in W/(mK). Huber et al. [1] use the value 1.32×10^{-3}, corresponding to the modified Eucken correlation. Reid et al. [5] review this factor and state that even the value of 1×10^{-3} is too high for polar fluids. They review five different interpretations of f_{int}, but most of these involve quantities which are not available for many fluids. They also demonstrate that this factor has a weak, nearly linear, temperature dependence for a wide variety of fluids. Therefore, we take this factor to be an adjustable parameter and fit it to low-density experimental data as a linear function of temperature. In the absence of data, we use the constant 1.32×10^{-3}.

The dilute-gas part of the translational term is given by

$$\lambda_j^*(T) = \frac{15R\eta_j^*(T)}{4M_j}. \tag{4}$$

The dilute-gas viscosity appearing in Eqs. (3) and (4) is given by standard kinetic gas theory [4]:

$$\eta_j^*(T) = 26.69\times10^{-3}\frac{(M_jT)^{1/2}}{\sigma_j^2\Omega^{(2,2)}(kT/\varepsilon_j)} \tag{5}$$

where σ_j (in nm) and ε/k (in kelvins) are the molecular size and energy parameters associated with an intermolecular potential function, such as the Lennard–Jones 12–6 potential, and $\Omega^{(2,2)}$ is the collision integral (again for the Lennard–Jones fluid), which is a function of the temperature and $\frac{\varepsilon}{k}$. We use the empirical function of Neufeld et al. [6] for $\Omega^{(2,2)}$. While Eq. (5) is derived from theory, the molecular size and energy parameters are most often evaluated from low-density viscosity data. This function can thus be treated as a theoretically based correlating function.

Where experimentally based Lennard–Jones parameters are not available, they may be estimated by the relations suggested by Huber and Ely [7]:

$$\varepsilon_j/k = \varepsilon_0/k\frac{T_j^{\text{crit}}}{T_0^{\text{crit}}}, \text{ and} \tag{6}$$

$$\sigma_j = \sigma_0\left(\frac{\rho_0^{\text{crit}}}{\rho_j^{\text{crit}}}\right)^{1/3} \tag{7}$$

where the subscript 0 refers to the reference fluid used in the extended corresponding states method described below.

2.2. Residual (density-dependent) contribution

We use the principle of corresponding states to model the residual part of the thermal conductivity. Such models have been applied to a wide variety of fluids by many authors, including Leland and Chappelear [8], Hanley [9], Ely and Hanley [3], and Huber et al. [1]. This approach is especially useful for fluids with limited experimental data.

The simple corresponding states model is based on the assumption that different fluids are conformal; that is, they obey, in reduced coordinates, the same intermolecular force laws. (A reduced property is obtained by dividing by its value at the critical point.) This

assumption leads to the conclusion that, with the appropriate scaling of temperature and density, the reduced residual Helmholtz energies and compressibilities of the unknown fluid "j" and a reference fluid "0" (for which an accurate, wide-ranging equation of state is available) are equal:

$$\alpha_j^{\mathrm{r}}(T,\rho) = \frac{A_j(T,\rho) - A_j^*(T,\rho)}{RT} = \alpha_0^{\mathrm{r}}(T_0,\rho_0), \tag{8}$$

and

$$Z_j(T,\rho) = Z_0(T_0,\rho_0). \tag{9}$$

The reference fluid is chosen to provide the best fit of the data and usually has a molecular structure similar to the fluid of interest.

The "conformal" temperature and density T_0 and ρ_0 defined by Eqs. (8) and (9) are related to the actual T and ρ of the fluid of interest by

$$T_0 = \frac{T}{f} = T\frac{T_0^{\mathrm{crit}}}{T_j^{\mathrm{crit}}\theta(T,\rho)}, \tag{10}$$

and

$$\rho_0 = \rho h = \rho\frac{\rho_0^{\mathrm{crit}}}{\rho_j^{\mathrm{crit}}}\phi(T,\rho), \tag{11}$$

where the multipliers $1/f$ and h are termed equivalent substance reducing ratios, or simply "reducing ratios." Initially, the corresponding states approach was developed for spherically symmetric molecules for which the reducing ratios are simple ratios of the critical parameters (θ and ϕ both equal to 1). The extended corresponding states (ECS) model extends the method to other types of molecules by the introduction of the "shape factors" θ and ϕ. These shape factors are functions of temperature and density, although often the density dependence is neglected.

The ECS method has been applied to both the thermodynamic and transport properties. By analogy with the thermodynamic properties, the thermal conductivity would be given by

$$\lambda_j^{\mathrm{r}}(T,\rho) = \lambda_0^{\mathrm{r}}(T_0,\rho_0)\frac{\lambda_j(T_j^{\mathrm{crit}},\rho_j^{\mathrm{crit}})}{\lambda_0(T_0^{\mathrm{crit}},\rho_0^{\mathrm{crit}})}. \tag{12}$$

But the thermal conductivity approaches infinity at the critical point, and thus, another reducing parameter must be found. Evaluating the translational contribution given by kinetic theory [Eqs. (4) and (5)] at the critical temperature yields

$$\lambda_j^*(T_j^{\mathrm{crit}}) = \frac{C}{\sigma_j^2\Omega^{(2,2)}(T_j^{\mathrm{crit}}k/\varepsilon_j)}\left(\frac{T_j^{\mathrm{crit}}}{M_j}\right)^{1/2}, \tag{13}$$

where the gas constant and numerical constants in Eqs. (4) and (5) have been merged into the constant C. This reducing parameter has no physical meaning in itself, but it does have a reasonable theoretical basis.

Combining the reducing parameter defined in Eq. (13) with Eq. (12) yields

$$\lambda_j^{\mathrm{r}}(T,\rho) = \lambda_0^{\mathrm{r}}(T_0,\rho_0)\left(\frac{T_j^{\mathrm{crit}}}{T_0^{\mathrm{crit}}}\right)^{1/2}\frac{\sigma_0^2\Omega^{(2,2)}(T_0^{\mathrm{crit}}k/\varepsilon_0)}{\sigma_j^2\Omega^{(2,2)}(T_j^{\mathrm{crit}}k/\varepsilon_j)} \times\left(\frac{M_0}{M_j}\right)^{1/2}. \tag{14}$$

If the molecular size parameter σ is taken to be proportional to the cube root of the critical volume, and the collision integrals $\Omega^{(2,2)}$ are assumed to be equal for fluid j and the reference fluid at their respective critical temperatures [reasonable assumptions in view of Eqs. (6) and (7)], we obtain

$$\lambda_j^{\mathrm{r}}(T,\rho) = \lambda_0^{\mathrm{r}}(T_0,\rho_0)\left(\frac{T_j^{\mathrm{crit}}}{T_0^{\mathrm{crit}}}\right)^{1/2}\left(\frac{\rho_j^{\mathrm{crit}}}{\rho_0^{\mathrm{crit}}}\right)^{2/3}\left(\frac{M_0}{M_j}\right)^{1/2}. \tag{15}$$

Finally, if the ratios of critical parameters in Eq. (15) are replaced by the reducing ratios in Eqs. (10) and (11), we obtain

$$\lambda_j^{\mathrm{r}}(T,\rho) = \lambda_0^{\mathrm{r}}(T_0,\rho_0)F_\lambda, \tag{16}$$

where

$$F_\lambda = f^{1/2}h^{-2/3}\left(\frac{M_0}{M_j}\right)^{1/2} \tag{17}$$

This result is equivalent to Eqs. (11) and (12) of Huber et al. [1]. Note that the dependence on the molar masses is the inverse of the corresponding expression for viscosity [Eq. (5) in [7] or Eq. (11) in [2]].

The shape factors (or, equivalently, the reducing ratios) may be obtained in several different ways. They can be fitted to experimental data, most often to vapor pressures and saturated-liquid densities. There are predictive methods which do not require any experimental data. In this work, we use the "exact shape factor" method [10], where one equation of state is mapped onto another; that is, the conformal temperature and density which satisfy Eqs. (8) and (9) are found directly. The exact shape factor method implicitly assumes that accurate equations of state are available for both fluid j and the reference fluid.

Numerical solution of Eqs. (8) and (9) to find the reducing ratios is straightforward in principle but somewhat complicated in practice. At moderate and high densities, a standard two-dimensional Newton's method iteration is used. The standard method is constrained in two ways. First, the derivative $(\partial P/\partial\rho)_T$ is

calculated, and if it is negative (corresponding to an unstable thermodynamic state), a different guess for density or temperature is generated. Second, the size of the temperature and density steps between iterations is limited. At low densities, this system tends towards a singularity, and a solution may not exist. If the Newton's method iteration fails, the quantity X, defined by

$$X = \left[\alpha_j^{\mathrm{r}}(T,\rho) - \alpha_0^{\mathrm{r}}(T_0,\rho_0)\right]^2 + \left[Z_j(T,\rho) - Z_0(T_0,\rho_0)\right]^2, \tag{18}$$

is minimized. The density which minimizes X is found using a Brent's method parabolic interpolation scheme [11]. For each trial value of ρ_0 a secant method iteration is used to find the T_0 which satisfies Eq. (8).

2.3. Modification of the pure-fluid ECS method of Huber et al.

In view of the assumptions made in the ECS method, it is not apparent that the reducing ratios calculated from a thermodynamic equation of state should apply equally well to the transport properties. Klein et al. [2] have shown that adjusting the conformal density by the addition of a viscosity shape factor improves the accuracy of the ECS method for that property. This approach can be extended to thermal conductivity as well by introducing a thermal conductivity shape factor χ defined by

$$\rho_0 = \chi h \rho, \tag{19}$$

where χ is a simple function of reduced density:

$$\chi = \sum_{k=0}^{n} c_k (\rho/\rho^{\mathrm{crit}})^k. \tag{20}$$

The shape factor χ adjusts the conformal density at which the reference fluid thermal conductivity formulation is evaluated. If there were an exact correspondence between the thermodynamic properties and thermal conductivity, χ would be 1 for all fluids and at all conditions. We apply this new shape factor to a variety of fluids and demonstrate that values different from 1 improve the representation of experimental data.

2.4. Critical enhancement

The thermal conductivity approaches infinity at the critical point, and even well removed from the critical point this "critical enhancement" can be a significant portion of the total thermal conductivity. Huber et al. [1] apply the same multiplier F_λ to both the residual and critical enhancement parts of the reference fluid thermal conductivity. Although the theoretical basis for this approach is weak, it works fairly well empirically. They evaluate the critical enhancement at the same conformal temperature and density as the residual part. This has the small, but disconcerting, problem that the maximum in the critical enhancement for fluid j will not occur at the critical point unless the shape factors are both 1.

To locate the critical enhancement correctly, we propose evaluating that term for the reference fluid at the same reduced temperature as the fluid of interest. In other words, for the critical enhancement only, the conformal temperature and density are

$$T_0^{\mathrm{c.e.}} = \frac{T}{T_j^{\mathrm{crit}}} T_0^{\mathrm{crit}} \tag{21}$$

and

$$\rho_0^{\mathrm{c.e.}} = \frac{\rho}{\rho_j^{\mathrm{crit}}} \rho_0^{\mathrm{crit}}, \tag{22}$$

where the superscript "c.e." indicates that these conformal conditions apply only to the critical enhancement term.

While this modification correctly places the singularity in the thermal conductivity at the critical point it introduces a different problem. Far from critical, the simple reduced temperature and density are sometimes inside the two-phase boundary of the reference fluid, with the result that the critical enhancement is incorrect or even of the wrong sign. (The reference fluid formulation we employ requires the evaluation of $(\partial P/\partial\rho)_T$, and this quantity can be zero or negative inside the two-phase region.)

To avoid both these problems, we propose the following method. The conformal conditions for the critical enhancement are the reduced conditions [Eqs. (21) and (22)] at the critical point. For $0.8\,T^{\mathrm{crit}} < T < 1.2\,T^{\mathrm{crit}}$ and $0.6\rho^{\mathrm{crit}} < \rho < 1.4\,\rho^{\mathrm{crit}}$ they approach the "normal" conformal conditions [Eqs. (10) and (11)] in a linear fashion. While this method is completely empirical, it is reasonably accurate in representing the critical region data as demonstrated below.

2.5. Reference fluid formulation

Refrigerant 134a (1,1,1,2-tetrafluoroethane) was used in this work as the reference fluid. An extensive body of recent, high-quality experimental data is available for this fluid. It is a polar hydrofluorocarbon and is, thus, chemically similar to the other new HFC refrigerants, including R32, R125, and R143a. We use the recent R134a thermal conductivity surface of Perkins et al. [12], which is based on data measured in an IUPAC-sponsored evaluation [13]. The thermodynamic properties are calculated with the equation of state of Tillner-Roth and Baehr [14].

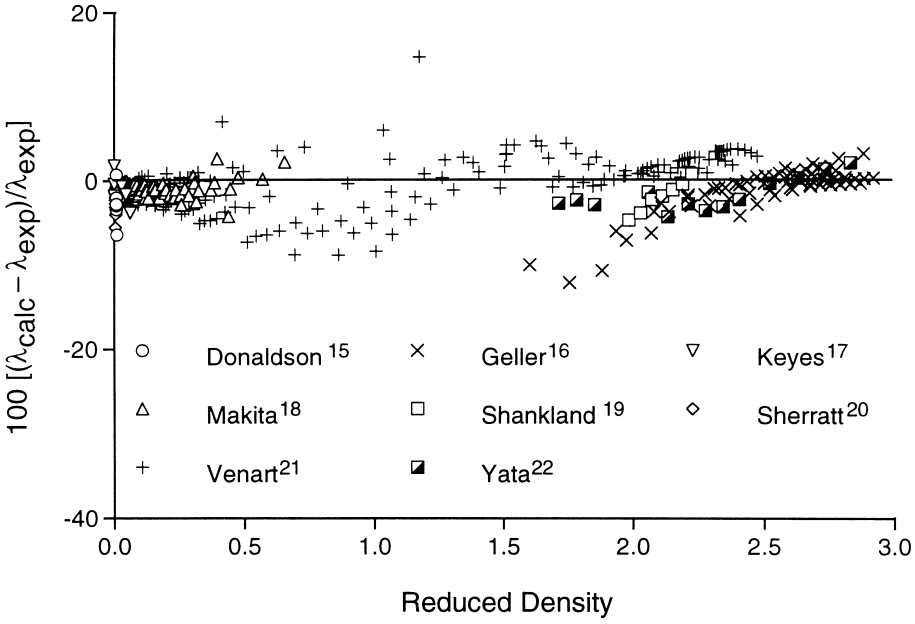

Fig. 1. Deviations between experimental thermal conductivity data for R12 and values calculated with the "traditional" ECS method [$f_{int} = 1.32 \times 10^{-3}$, $\chi = 1$].

Fig. 1. Déviations entre les données de conductivité thermique pour le R12 et valeurs calculées utilisant la méthode « traditionnelle » ECS [f_{int} = 1,32 x 10^{-3}, χ = 1].

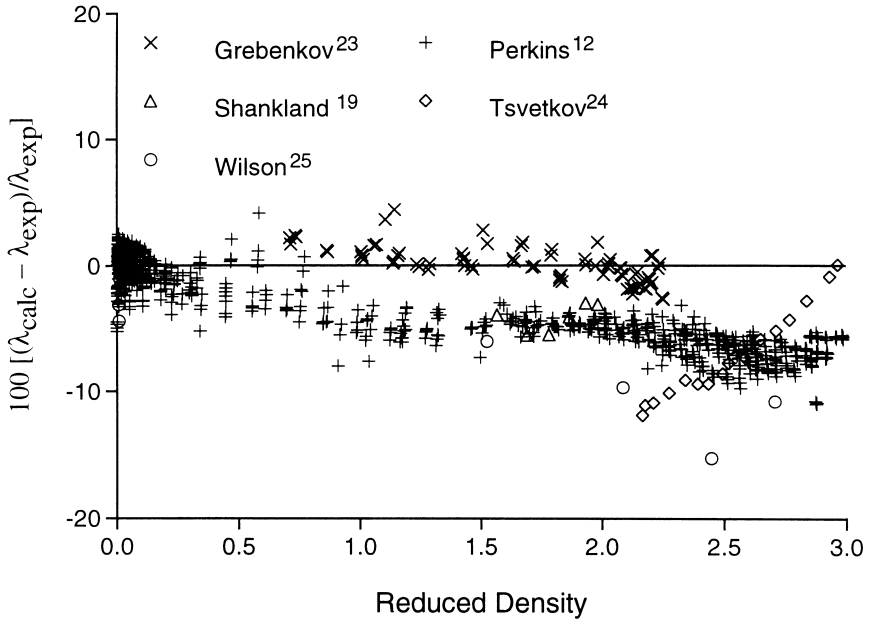

Fig. 2. Deviations between experimental thermal conductivity data for R125 and values calculated with the "traditional" ECS method [$f_{int} = 1.32 \times 10^{-3}$, $\chi = 1$].

Fig. 2. Déviations entre les données de conductivité thermique pour le R125 et valeurs calculées utilisant la méthode « traditionnelle » ECS [f_{int} = 1,32 x 10^{-3}, χ = 1].

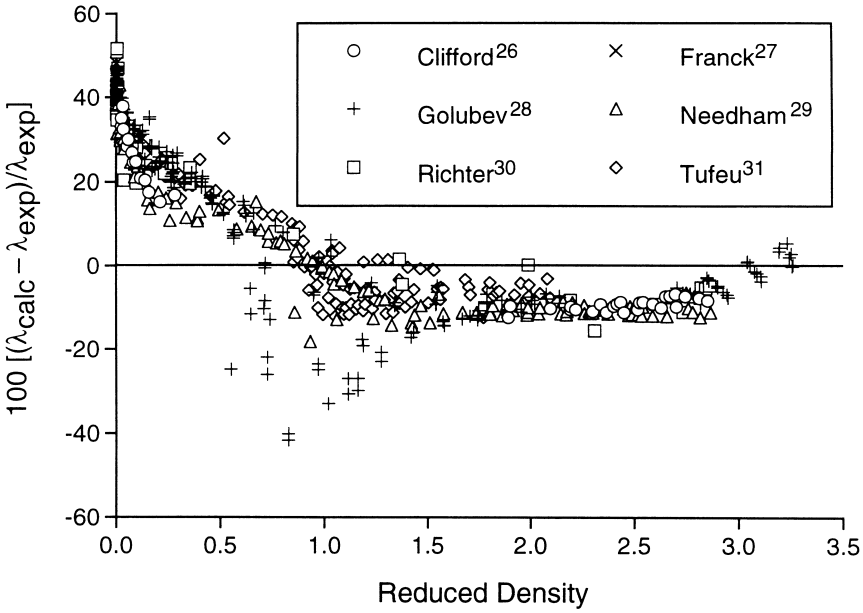

Fig. 3. Deviations between experimental thermal conductivity data for ammonia and values calculated with the "traditional" ECS method [$f_{int} = 1.32 \times 10^{-3}$, $\chi = 1$].

Fig. 3. Déviations entre les données de conductivité thermique pour l 'ammoniac et valeurs calculées utilisant la méthode « traditionnelle » ECS [f_{int} = 1,32 x 10^{-3}, χ = 1].

2.6. Pure fluid results

Thermal conductivity values computed with the ECS method are compared to experimental values for R12, R125, and ammonia in Figs. 1–3. Although a major motivation for the ECS method is the calculation of properties for fluids with limited data, it is instructive to compare the method for fluids with extensive data sets available. In these three figures, f_{int} is taken to be 1.32×10^{-3} and the thermal conductivity shape factor is taken to be 1, corresponding to the Huber et al. [1] method (except for the minor difference in the conformal conditions at which the critical enhancement is evaluated, as discussed above). For R12, this, the "traditional" ECS method, is seen to work very well. At high densities, the deviations are clustered about 0 and their magnitudes are only slightly larger than the differences between different data sets. The deviations as the density approaches 0 are less than 4%, but systematically negative, indicating that the modified Eucken correlation adequately describes the dilute-gas region, but could be improved by an optimized f_{int}. The deviations increase at densities near critical. The good quality of the fit is indicated by an overall average absolute deviation of 1.64%, where

$$AAD = \frac{1}{n_{points}} \sum_{k=1}^{n_{points}} 100 \left| \frac{\lambda_{calc} - \lambda_{exp}}{\lambda_{exp}} \right|. \quad (23)$$

For R125 (Fig. 2), the scatter at the dilute-gas limit is slightly larger. At higher densities, a systematic deviation of as much as 8% is seen. The overall AAD is 3.02%.

For ammonia (Fig. 3), the dilute-gas values are overpredicted by as much as 50%, confirming the statement of Reid et al. [5] that the f_{int} in the Eucken correlation is too high for polar fluids. Near the critical density, a few points show deviations as high as 40%. At higher densities, the calculated values are consistently low by about 10%. The overall AAD is 17.4%.

The results for the "traditional" ECS method for a variety of fluids commonly used as refrigerants are summarized by the average absolute deviations given in the penultimate column of Table 1. (The data sources used in this work were selected to cover a wide range of temperature and density. We consider them reliable sources, but the listing in Table 1 is not intended to be a comprehensive literature survey of the available data.) The HFCs, HCFCs, CFCs, hydrocarbons, ammonia, and carbon dioxide considered here represent a wide range of polarities and molecular sizes and structures, yet the traditional ECS method does a commendable job of representing thermal conductivity for most of these fluids. Even for ammonia, the fluid showing the largest deviations, the AAD of 17.4% is not large considering that ammonia has a thermal conductivity as much as 6 times that of the reference fluid, and nearly half the overall AAD is due to a deficiency in the dilute-gas portion of the calculation. Recall that these results

Table 1
Data sources and average absolute deviations between experimental data and values computed with the "traditional" ECS method [$f_{int} = 1.32 \times 10^{-3}$, $\chi = 1$] and the present model [$f_{int} = f(T)$, $\chi = f(\rho/\rho^{crti})$]

Tableau 1
Sources des données et déviations absolues moyennes entre les valeurs expérimentales moyennes absolues et les valeurs calculées selon la méthode ECS traditionnelle précédente [f_{int} = 1,32 x 10^{-3}, x = 1] et le modèle utilisé dans cette étude [$f_{int} = f(T)$, $x = f(\rho/\rho^{crti})$]

Fluid	Equation of state source	Data source	No. points	Data range		AAD (%)	
				T (K)	ρ/ρ^{crit}	Traditional method	Present model
Ammonia	Tillner-Roth et al. [32]	Clifford and Tufeu [26]	40	296–387	0.025–2.84	15.20	3.16
		Franck [27]	7	275–584	0.0005–0.0011	42.32	1.85
		Golubev and Sololova [28]	237	206–773	0.0012–3.25	21.41	4.52
		Needham and Ziebland [29]	115	294–450	0.0038–2.86	13.87	4.25
		Richter and Sage [30]	38	278–478	0.0020–2.85	22.16	4.81
		Tufeu at al. [31]	122	381–578	0.016–2.09	10.88	5.19
		Fluid totals	559	199–773	0.0005–3.25	17.43	4.50
CO_2	Ely et al. [33]	Johns et al. [34]	33	381–474	0.045–1.19	4.65	0.90
		Johnston and Grilly [35]	11	186–379	0.0002–0.0003	7.29	0.46
		Millat et al. [36]	91	305–426	0.015–0.38	4.19	1.31
		Scott et al. [37]	92	301–350	0.011–1.85	7.54	2.09
		Fluid totals	227	186–474	0.0002–1.85	5.76	1.53
Propane	Younglove and Ely [38]	Aggarwal and Springer [39]	30	400–600	0.0040–0.038	3.35	2.89
		Mann and Dickins [40]	36	275–283	0.002–0.0087	7.12	0.23
		Roder [41]	283	168–301	2.22–3.09	12.44	1.18
		Tufeu and LeNeindre [42]	174	296–579	0.042–2.53	10.26	3.13
		Fluid totals	523	168–600	0.0022–3.09	10.83	1.86
R11	Jacobsen et al. [43]	Richard and Shankland [44]	6	305–328	0.0094–0.010	4.54	1.19
		Shankland [19]	14	305–341	0.0094–2.62	3.78	0.96
		Yata et al. [22]	12	233–438	1.84–2.93	4.26	1.16
		Fluid totals	32	233–438	0.0094–2.93	4.10	1.08
R12	Marx et al. [45]	Donaldson [15]	6	277–347	0.0076–0.0096	2.98	2.18
		Geller et al. [16]	65	193–373	1.60–2.92	1.81	1.86
		Keyes [17]	7	323–423	0.0000–0.062	1.75	1.36
		Makita et al. [18]	68	298–393	0.0066–0.66	0.99	0.73
		Shankland [19]	13	303–343	0.0081–2.22	2.18	1.70
		Sherratt and Giffits [20]	6	306–489	0.0053–0.0087	2.27	1.55
		Venart and Mani [21]	204	300–600	0.0044–2.47	1.66	1.29
		Yata et al. [22]	13	204–366	1.71–2.83	2.20	2.32

Table 1 (*continued*)
Tableau 1 (*suite*)

Fluid	Equation of state source	Data source	No. points	Data range		AAD (%)	
				T (K)	ρ/ρ^{crit}	Traditional method	Present model
		Fluid totals	382	193–600	0.0000–2.92	1.64	1.36
R13	Platzer et al. [46]	Geller and Peredrii [47]	78	213–433	0.0051–2.79	5.39	3.42
		Makita et al. [18]	126	283–373	0.0059–1.56	6.60	3.27
		Yata et al. [22]	4	204–264	2.05–2.57	0.79	2.35
		Fluid totals	208	204–433	0.0051–2.79	6.03	3.31
R22	Kamei et al. [48]	Assael and Karagiannidis [49]	37	253–333	1.98–2.67	5.22	0.73
		Donaldson [15]	5	290–351	0.0058–0.0071	4.63	6.53
		Makita et al. [18]	130	298–393	0.0051–1.30	3.32	1.99
		Shankland [19]	4	312–342	1.87–2.16	2.08	3.42
		Tsvetkov and Laptev [50]	134	313–411	0.0050–2.19	6.37	6.18
		Yata et al [22]	6	234–345	1.68–2.68	3.76	1.23
		Fluid totals	316	234–411	0.0050–2.68	4.85	3.70
R23	ECS model in McLinden et al. [51]	Geller and Peredrii [47]	80	193–433	0.20–2.93	6.08	3.84
		Makita et al. [18]	102	283–373	0.0000–0.78	4.16	1.45
		Fluid totals	182	193–433	0.0000–2.93	5.00	2.50
R32	Tillner-Roth and Yokozeki [52]	Grebenkov et al. [23]	72	275–403	0.69–2.53	3.88	9.62
		Perkins et al. [12]	1605	161–405	0.0017–3.35	10.51	3.17
		Fluid totals	1677	161–405	0.0017–3.35	10.23	3.45
R114	Platzer et al. [46]	Donaldson [15]	4	304–343	0.011–0.012	9.29	9.27
		Keyes [17]	3	323–423	0.0086–0.011	1.90	1.89
		Shankland [19]	7	309–341	2.26–2.45	3.88	1.29
		Yata et al. [22]	6	224–387	0.0000–2.59	3.00	1.19
		Fluid totals	20	224–423	0.0000–2.71	4.40	2.95
R115	ECS model in McLinden et al. [51]	Yata et al. [22]	7	234–320	1.89–2.54	4.37	1.19
		Hahne et al. [53]	163	290–369	0.021–2.22	7.06	5.76
		Fluid totals	170	234–369	0.021–2.54	6.95	5.57
R125	Outcalt and McLinden [54]	Grebenkov et al. [23]	74	295–403	0.71–2.25	1.07	4.34
		Perkins et al. [12]	978	192–392	0.0019–2.98	3.06	1.00
		Shankland [19]	6	307–332	1.56–1.98	4.17	1.28
		Tsvetkov et al. [24]	16	173–290	2.16–2.96	7.14	3.99
		Wilson et al. [25]	7	216–333	0.0078–2.71	7.17	4.38

(continued on next page)

Table 1 (*continued*)
Tableau 1 (*suite*)

Fluid	Equation of state source	Data source	No. points	Data range		AAD (%)	
				T (K)	ρ/ρ^{crit}	Traditional method	Present model
		Fluid totals	1081	173–403	0.0019–2.98	3.02	1.30
R142b	ECS model in McLinden et al. [51]	Perkins et al. [55]	56	302–304	2.53–2.87	4.45	0.89
		Sousa et al. [56]	164	290–515	0.026–2.71	4.38	2.55
		Tanaka et al. [57]	21	293–353	0.0088–0.14	1.55	1.76
		Yata et al. [58]	24	251–333	2.35–2.93	6.84	1.91
		Fluid totals	265	251–515	0.0088–2.93	4.39	2.08
R143a	Outcalt and McLinden [59]	Perkins, data published in [60] (steady state)	119	191–371	0.0001–0.095	6.68	1.91
		Perkins, data published in [60] (transient)	1125	191–373	0.0012–3.07	4.89	2.80
		Tanaka et al. [57]	30	293–353	0.0067–0.58	7.27	14.01
		Yata et al. [58]	24	268–314	2.07–2.64	9.64	4.00
		Fluid totals	1298	191–373	0.0001–3.07	4.49	3.00

are purely predictive — they are not dependent on any experimental thermal conductivity values (apart from those underlying the reference fluid formulation).

When experimental data are available, they can be used to adjust the f_{int} and/or χ and improve the calculated values. For R125, the systematic underprediction at high densities can be avoided by adjusting the thermal conductivity shape factor χ. This was done by finding, for each data point, the value of χ at which the calculated and experimental values of thermal conductivity agree using a Fibonnaci search technique. The resulting values of χ are shown in Fig. 4. At high densities, the optimum values of χ are tightly clustered about an average value of about 1.03. At low densities, the scatter increases dramatically. Several points did not converge at all and are plotted at the iteration bounds of 0 and 2. Since the χ shape factor affects only the residual part of the thermal conductivity, and at low densities, this term is a small fraction of the total, this scatter merely indicates that a large change in the residual term would be needed to compensate for small errors in the dilute-gas term. Using a χ which is a linear function of reduced density, together with an adjusted f_{int} results in the deviations shown in Fig. 5. The overall AAD has been reduced from 3.02 to 1.30%.

For ammonia, the optimum values of f_{int} were found in the same manner as that used for χ, except that only data points at $\rho/\rho^{crit} < 0.01$ were used. The resulting values of f_{int} were fitted as a linear function of temperature, as shown in Fig. 6. Using this function for f_{int}, the optimum χ values were then found, and a quadratic function was fitted to points at $\rho/\rho^{crit} > 1$. The resulting deviations are shown in Fig. 7. The thermal conductivity is calculated over the full range of density with an AAD of 4.50%.

Refrigerant 12, which was represented very well by the traditional ECS method, and ammonia, which showed a dramatic improvement with the modified method, represent the extremes. Intermediate results were obtained for the other fluids considered. Table 2 gives the optimized f_{int} functions as well as the values and sources for the molecular size and energy parameters. Table 3 gives the coefficients to the χ function [Eq. (20)]. The final column in Table 1 gives the AAD using these optimized functions for f_{int} and χ.

3. Thermal conductivity of mixtures

3.1. Dilute-gas contribution

The thermal conductivity of a mixture is composed of the same four terms seen in Eq. (2). Reid et al. [5] and Mason and Uribe [67] refer to numerous papers which derive the thermal conductivities of dilute-gas mixtures from kinetic theory. Mason and Uribe [67] point out, however, that the theoretical expressions "are very

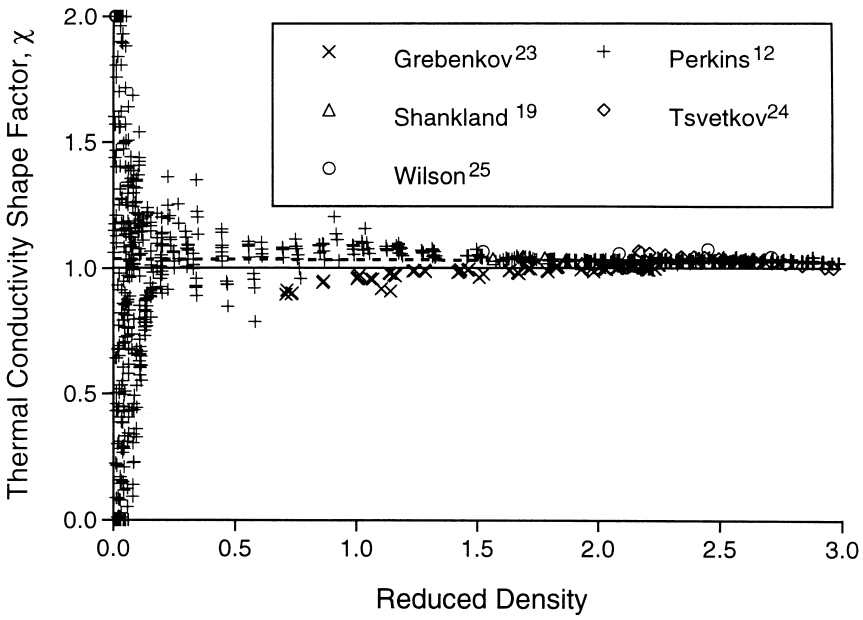

Fig. 4. Values of the thermal conductivity shape factor for R125 optimized for each data point. The solid line at $\chi = 1$ corresponds to the traditional ECS method; the dashed line is a least squares fit of the χ values at reduced densities >1.

Fig. 4. Valeurs du facteur de la forme de la conductivité thermique pour le R125 optimisée pour chaque donnée. La courbe continue à $\chi = 1$ correspond à la méthode traditionnelle ECS ; la courbe hachurée est obtenue avec la méthode des moindres carrés pour les valeurs de χ à densité réduite > 1.

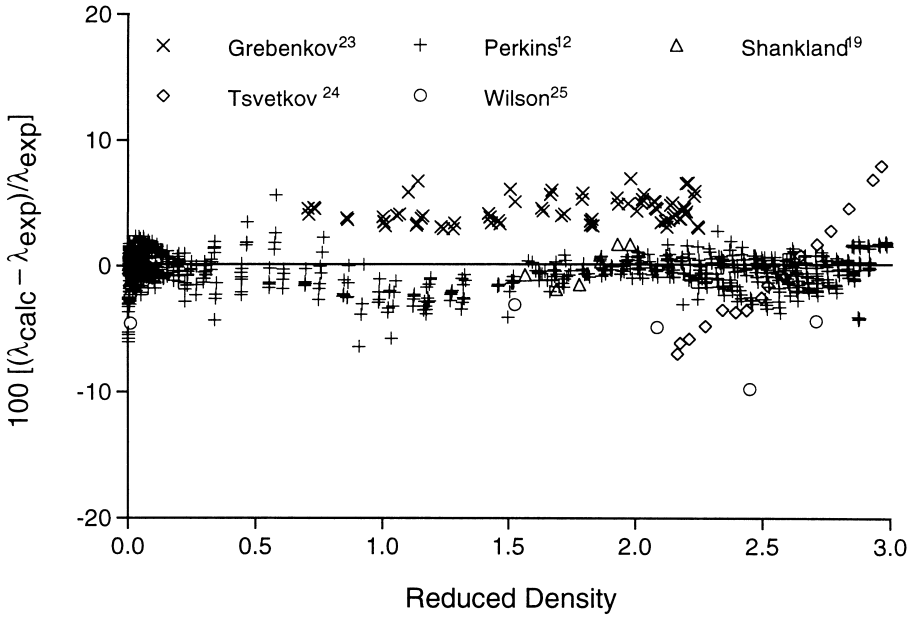

Fig. 5. Deviations between experimental thermal conductivity data for R125 and values calculated with the present ECS model [$f_{\text{int}} = f(T)$, $\chi = f(\rho/\rho^{\text{crit}})$].

Fig. 5. Déviations entre les données de conductivité thermique pour le R125 et valeurs calculées utilisant la méthode utilisée dans cette expérience : [$f_{int} = f(T)$, $\chi = f(\rho/\rho^{crti})$].

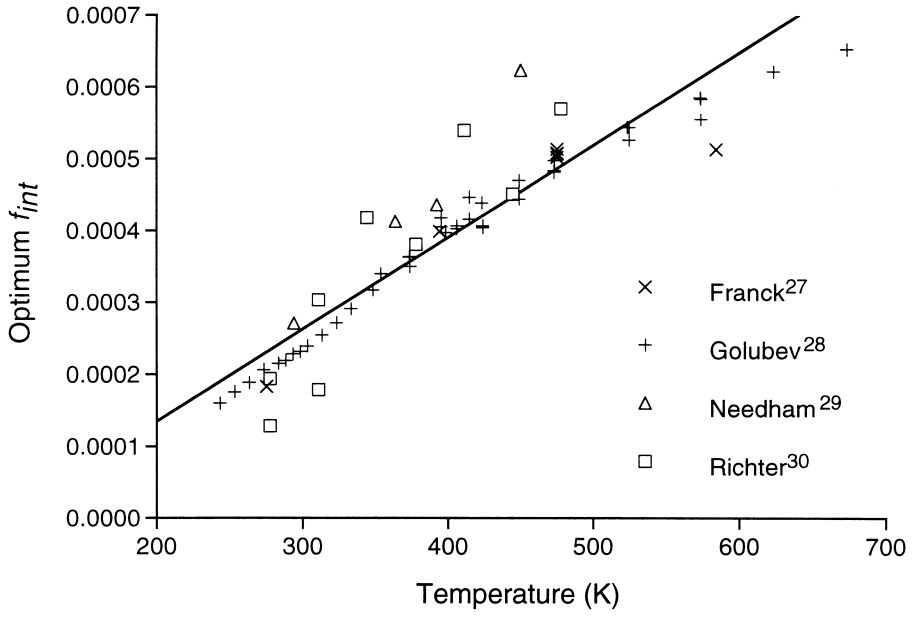

Fig. 6. Values of f_{int} optimized for individual data points for ammonia.

Fig. 6. Valeurs de f_{int} optimisées pour chaque donnée obtenue pour l'ammonia.

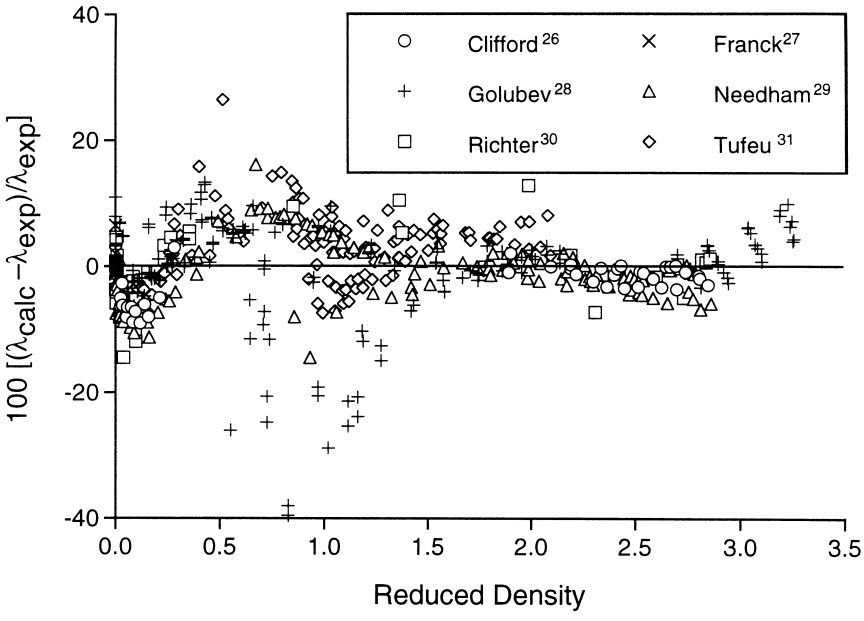

Fig. 7. Deviations between experimental thermal conductivity data for ammonia and values calculated with the present ECS model [$f_{\text{int}} = f(T)$, $\chi = f(\rho/\rho^{\text{crit}})$].

Fig. 7. Déviations entre les données de conductivité thermique pour l'ammoniac et valeurs calculées utilisant la méthode utilisée dans cette expérience : [$f_{int} = f(T)$, $\chi = f(\rho/\rho^{crti})$]

Table 2
Parameters for the dilute-gas thermal condictivity

Tableau 2
Paramètres pour la conductivité thermique de gaz dilués

	Molecular parameters			f_{int} in Eucken correlation [Eq. (3)]	
Fluid	Source	σ (nm)	ε/k (K)	Data source(s)	Functional from (T in kelvins)
Ammonia	Fenghour et al. [61]	0.2957	386.00	Clifford and Tufeu [26] Franck [27] Golubev and Sololova [28] Needham and Ziebland [29] Richter and Sage [30]	$-1.2172\times10^{-4}+1.2818\times10^{-6}\ T$
CO_2	Vesovic et al. [62]	0.3751	251.20	Johnston and Grilly [35] Millat et al. [36] Scott et al. [37]	$7.0793\times10^{-4}+1.3194\times10^{-6}\ T$
Propane	Vogel et al. [63]	0.4975	263.88	Mann and Dickins [40] Tufeu and LeNeindre [42]	$1.0398\times10^{-3}+5.4024\times10^{-7}\ T$
R11	[Eqs. (6) and (7)]	0.5447	363.61	Richard and Shankland [44]	1.4000×10^{-3}
R12	[Eqs. (6) and (7)]	0.5186	297.24	Donaldson [15] Keyes [17] Makita et al. [18] Shankland [19] Sherratt and Griffiths [20] Venart and Mani [21]	1.3440×10^{-3}
R13	[Eqs. (6) and (7)]	0.4909	233.36	Geller and Peredrii [47] Makita et al. [18]	1.3200×10^{-3}
R22	Takahashi et al. [64] [a]	0.4666	284.72	Donaldson [15] Makita et al. [18] Tsvetkov and Laptev [50]	$7.7817\times10^{-4}+1.2536\times10^{-6}\ T$
R23	[Eqs. (6) and (7)]	0.4430	230.83	Makita et al. [18]	$6.0570\times10^{-4}+1.8604\times10^{-6}\ T$
R32	Takahashi et al. [65] [a]	0.4098	289.65	Perkins et al. [12]	$8.1980\times10^{-4}+2.2352\times10^{-7}\ T$
R114	[Eqs. (6) and (7)]	0.5770	323.26	Donaldson [15] Keyes [17]	1.3200×10^{-3}
R115	[Eqs. (6) and (7)]	0.5476	272.53	Hahne et al. [53]	1.3200×10^{-3}
R125	Assael et al. [66] [a]	0.5101	261.39	Perkins et al. [12] Wilson et al. [25]	$1.2565\times10^{-3}+2.2296\times10^{-6}\ T$
R142b	[Eqs. (6) and (7)]	0.5320	316.64	Sousa et al. [56] Tanaka et al. [57]	1.3200×10^{-3}
R143a	[Eqs. (6) and (7)]	0.5025	267.10	Perkins, data published in [60] Tanaka et al. [57]	$1.0066\times10^{-3}+1.3729\times10^{-6}\ T$

[a] Molecular parameters fitted to the low-density viscosity data of the listed source.

complicated and contain many essentially unknown quantities…" They go on to state "Direct use of these formulas is essentially hopeless." Reid et al. [5] observe that mixtures having components of greatly differing polarities generally exhibit a thermal conductivity greater than a simple mole-fraction average, while non-polar systems exhibit the opposite trend, especially when the molecular sizes of the components differ.

In view of this rather distressing lack of theoretical guidance, and after comparing several mixing rules to the data of Perkins et al. [68,69], we represent the internal and translational contributions with the empirical mixing rule of Mason and Saxena [70], which is a modification of the Wassiljewa [71] equation:

$$\lambda^{\text{int}}_{\text{mix}}(T,x)+\lambda^{*}_{\text{mix}}(T,x)=\sum_{j=1}^{n}\frac{x_j[\lambda^{\text{int}}_{j}(T)+\lambda^{*}_{j}(T)]}{\sum_{i=1}^{n}x_i\phi_{ji}} \tag{24}$$

Table 3
Coefficients for the thermal conductivity shape factor [Eq. (20)]; coefficients not listed are 0

Tableau 3
Coefficients du facteur de forme de la conductivité thermique [Eq. (20)] ; les coefficients n'y figurant pas sont représentés par 0

Fluid	c_0	c_1	c_2	c_3
Ammonia	1.4312	−0.2326400	0.032521	
CO_2	0.8998	0.0297332		
Propane	0.8148	0.0510390		
R11	1.0724	−0.0226720		
R12	0.9910	0.0029509		
R13	1.4078	−0.2634600	0.037978	
R22	1.0750	−0.0385740		
R23	1.3801	−0.2797500	0.048798	
R32	1.2325	−0.0883940		
R114	1.0961	−0.0348990		
R115	1.0338	−0.0020661		
R125	1.0369	−0.0030368		
R142b	1.6808	−0.8395440	0.321957	−0.039706
R143a	1.1779	−0.2054100	0.064870	−0.006473

where

$$\phi_{ji} = \frac{\left[1 + \left(\eta_j^*/\eta_i^*\right)^{1/2}\left(M_j/M_i\right)^{1/4}\right]^2}{\left[8\left(1 + M_j/M_i\right)\right]^{1/2}}, \tag{25}$$

x is the molar composition for the n component mixture, and η_j^* is the dilute gas viscosity given by Eq. (4). All quantities in the dilute-gas terms are evaluated at the temperature of the mixture, rather than some conformal temperature.

3.2. Residual (density-dependent) contribution

The residual part of the mixture thermal conductivity is modeled with the extended corresponding states method. Following Huber et al. [1], we replace the ratio of molar masses appearing in Eq. (17) with a "mass reducing ratio" g_x, so that

$$F_\lambda = f_x^{1/2} h_x^{-2/3} g_x^{1/2}, \tag{26}$$

where the subscript x indicates a mixture quantity and

$$g_x^{1/2} = \frac{M_0^{1/2}}{f_x^{1/2} h_x^{4/3}} \sum_{i=1}^{n}\sum_{j=1}^{n} x_i x_j (f_i f_i)^{1/4} \left(\frac{2}{1/g_i + 1/g_j}\right)^{-1/2} \times \left[\frac{1}{8}\left(h_i^{1/3} + h_j^{1/3}\right)^3\right]^{4/3}. \tag{27}$$

At least three analogous expressions for g_x have appeared in the literature [3,72,73]. They differ in the exponents on the terms. We think that Eq. (27), which derives from the original expression of Ely and Hanley [72], has the best theoretical basis of the three [74].

Huber et al. [1] set $g_i = M_i$ in Eq. (27). In an extension to their method, we define the g_i in a manner analogous to our earlier work on viscosity [2]:

$$g_i = M_0 \left[\frac{\lambda_0^{\mathrm{r}}(T_0, \rho_0)}{\lambda_j^{\mathrm{r}}(T_j, \rho_j)}\right]^2 f_j h_j^{-4/3}. \tag{28}$$

As with viscosity, this modification allows the use of a fluid-specific correlation for the thermal conductivity of the components, if one is available.

The reducing ratios f_j, h_j, f_x, and h_x for the components and mixture appearing in Eqs. (27) and (28) (or, equivalently, the conformal temperatures and densities) may be calculated in a variety of ways. Friend and Ely [75] describe the system of simultaneous equations and mixing rules needed to calculate the reducing ratios when the ECS model is used for calculating both the thermodynamic and transport properties of the mixture. Huber et al. [1] use the same method. If, however, a reliable equation of state is available for the mixture, the exact shape factor method may be used. We use the recent mixture Helmholtz energy model of Lemmon and Jacobsen [76,77]. The conformal conditions for component j and the mixture are found by solving the equations

$$\alpha_j^{\mathrm{r}}(T_j, \rho_j) = \alpha_{\mathrm{mix}}^{\mathrm{r}}(T, \rho, x), \tag{29}$$

$$Z_j(T_j, \rho_j) = Z_{\mathrm{mix}}(T, \rho, x), \tag{30}$$

$$\alpha_o^{\mathrm{r}}(T_0, \rho_0) = \alpha_{\mathrm{mix}}^{\mathrm{r}}(T, \rho, x), \tag{31}$$

and

$$Z_0(T_0, \rho_0) = Z_{\mathrm{mix}}(T, \rho, x). \tag{32}$$

The reducing ratios are then defined by

$$f_x = \frac{T}{T_0}, \tag{33}$$

$$h_x = \frac{\rho_0}{\rho}, \tag{34}$$

$$f_j = \frac{T_j f_x}{T}, \tag{35}$$

and

$$h_j = \frac{\rho h_x}{\rho_j}. \tag{36}$$

Table 4
Deviations between the mixture data of Perkins et al. [68,69] and values computed with the present ECS method

Tableau 4
Déviations entre les données sur les mélanges de Perkins et al. [68,69] et les valeurs calculées avec la méthode ECS utilisée dans cette étude

Mixture	Composition (mol fraction)	Data range		Number of points, AAD (%)									
		T (K)	ρ (mol/l)	Liquid (transient)		Vapor (transient)		Vapor (steady state)		Supercritical (transient)		Overall	
R125/134a	0.3002/0.6998	244–347	0.027–13.1	142	2.46	248	3.26	160	3.10			550	3.01
	0.7000/0.3000	247–344	0.034–12.4	136	4.87	202	2.43	205	2.28			543	2.98
R32/propane	0.2999/0.7001	229–347	0.012–14.2	159	5.15	139	8.00	225	11.41			523	8.60
	0.7001/0.2999	254–336	0.040–17.0	136	10.34	395	6.92	193	13.81			724	9.40
R32/134a	0.2996/0.7004	255–360	0.032–14.9	179	3.50	235	4.39	266	3.29			680	3.73
	0.7003/0.2997	254–348	0.033–18.1	130	6.25	231	5.38	267	5.03			628	5.40
Propane/R134a	0.2986/0.7014	250–348	0.057–11.9	246	2.97	233	4.00	235	4.58			714	3.84
	0.6997/0.3003	243–347	0.037–12.3	165	4.21	51	3.39	55	7.34			271	4.69
R32/125	0.5006/0.4994	190–344	0.014–18.6	406	7.36	965	4.03			296	4.77	1667	4.97
	0.8770/0.1230	190–343	0.091–23.8	543	2.29	1014	4.33					1557	3.62
R32/125/134a	0.333/0.333/0.334	250–344	0.033–14.7	175	10.02	81	5.41	107	4.33			363	7.31
	0.300/0.100/0.600	250–345	0.033–15.0	182	5.82	230	5.17	263	3.85			675	4.83

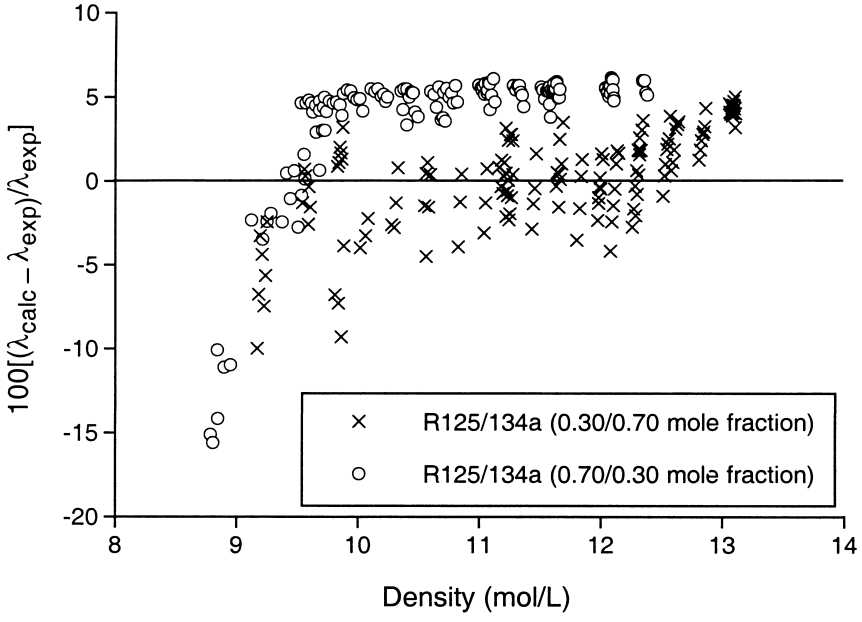

Fig. 8. Deviations between experimental thermal conductivity values in the liquid phase and values calculated with the present ECS model for two compositions of R125/134a.

Fig. 8. Déviations entre les valeurs expérimentales de conductivité thermique pour la phase liquide et les valeurs calculées à l'aide du modèle ECS utilisé dans cette étude pour les deux compositions de R125/R134a.

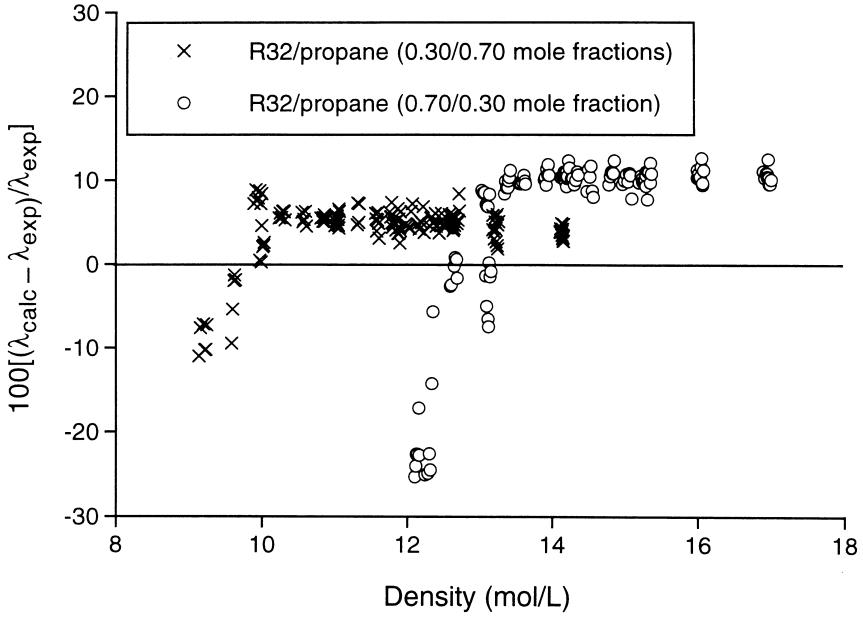

Fig. 9. Deviations between experimental thermal conductivity values in the liquid phase and values calculated with the present ECS model for two compositions of R32/propane.

Fig. 9. Déviations entre les valeurs expérimentales de conductivité thermique pour la phase liquide et les valeurs calculées à l'aide du modèle ECS utilisé dans cette étude pour les deux compositions de R32/propane.

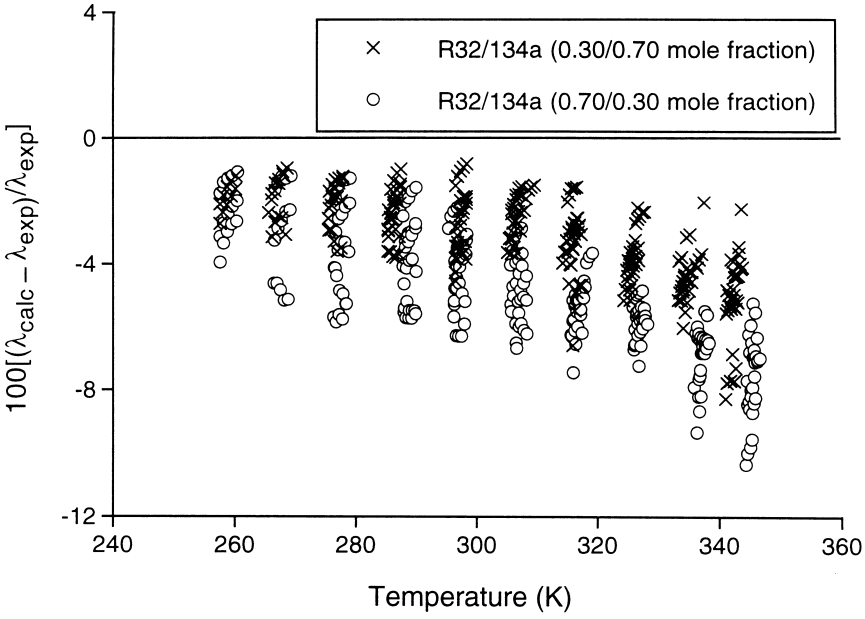

Fig. 10. Deviations between experimental thermal conductivity values in the vapor phase measured with the steady-state method and values calculated with the present ECS model for two compositions of R32/134a.

Fig. 10. Déviations entre les valeurs expérimentales de conductivité thermique pour la phase vapeur mesurées à l'aide de la méthode du régime permanent et les valeurs calculées à l'aide du modèle ECS utilisé dans cette étude pour les deux compositions de R32/R134a.

This exact shape factor method was that originally recommended by Ely and Hanley [10], but it has not usually been applied to mixtures for lack of a suitable mixture equation of state. These equations are solved using the same numerical scheme described above for the pure fluids. This method requires the solution of $(n+1)$ sets of two equations each, compared to the single, large system of $2n$ equations involved in the method described by Friend and Ely [75].

3.3. Critical enhancement

In the ECS method, the critical enhancement for a mixture is treated in the same fashion as a pure fluid. This results in the thermal conductivity of a mixture going to infinity at the mixture critical point, a result which is theoretically incorrect. However, Kiselev and Huber [78] demonstrate that the finite nature of the critical enhancement for mixtures is evident only in a very limited region around the critical point. This region varies in size from mixture to mixture but ranges from the order of one millikelvin (0.001 K) to a few kelvins above and below the critical temperature. In other words, the thermal conductivity of a mixture increases rapidly (in the same fashion as a pure fluid) as the critical point is approached and levels off very near the critical temperature. Considering that most vapor-compression refrigeration systems operate well away from the critical point, the incorrect behavior of the ECS model in this narrow region near the critical point is of little practical consequence.

3.4. Mixture results

The ECS method for mixtures is compared to recent data sets by Perkins et al. [68,69]. They measured thermal conductivities of 10 binary and two ternary mixtures containing R32, R125, R134a, and propane. The mixtures were prepared gravimetrically from the pure components for accurate knowledge of the composition. The measurements were carried out using transient and steady-state hot-wire methods. For most of the work, uninsulated tungsten hot wires (4 μm diameter) were used in transient and steady-state modes for measurements in the vapor phase. The extremely small wire diameter minimized corrections arising from a finite wire diameter. The steady-state technique allowed measurements at lower pressures than those possible with the transient method and also provided a cross check with the transient measurements. Anodized tantalum hot wires (25 μm diameter) were used in the transient mode for the liquid-phase measurements. The anodized layer of tantalum pentoxide provided the electrical insulation required for accurate measurements on the polar and moderately conducting HFCs. For the R32/125 mixtures, uninsulated platinum hot wires (12.7 μm diameter) were used in the transient mode for both the liquid and vapor measurements. The measurements cover the temperature range from 190 to 347 K over a wide range of densities. The total of 8895 measurements provide a consistent data set sufficient to test the validity of the mixture model.

A comparison of the experimental results with values calculated with the ECS model are given in Table 4. Separate statistics are reported for the transient liquid-phase, transient vapor-phase, steady-state vapor-phase, and supercritical results for each of the mixtures. Detailed liquid-phase comparisons for the R125/134a mixture (Fig. 8) show generally good agreement — the deviations are only slightly greater than the (2σ) experimental uncertainty of 3%. These deviations are greater for mixtures of polar and nonpolar fluids, such as the R32/propane mixture shown in Fig. 9. As the critical region is approached (towards the lower densities depicted in Figs. 8 and 9), the deviations increase for both systems.

In the vapor phase, the ECS model predicts values which are consistently low. The results for the R32/134a mixture shown in Fig. 10 are typical. The deviations are comparable to the experimental uncertainty at the lowest temperatures and increase as the critical temperature is approached. The transient and steady-state results are consistent. Higher deviations are seen with HFC + propane mixtures. These results confirm the observation of Reid et al. [5] that polar–nonpolar mixtures exhibit conductivities higher than a simple average.

4. Conclusions

The traditional ECS method of Huber et al. [1] works well in a purely predictive mode. The method predicts the thermal conductivities with an average absolute deviation of less than 7% (compared to experimental data over wide ranges of temperature and density) for 11 of the 14 fluids studied. The R134a reference fluid used in this method works quite well for a variety of fluids, not just other HFCs. Somewhat surprising was that the weakly polar CFCs, such as R12, showed some of the smallest deviations, even though the R134a reference fluid is a strongly polar HFC. This indicates that molecular geometry (which are similar for R12 and R134a) is the dominant influence in the ECS method rather than the polarity.

The present modification of the ECS method offers significant improvements over the traditional method for pure fluids when experimental thermal conductivity data are available. The relative improvement is greatest for highly polar fluids such as R32 and ammonia. Data at low densities are needed for polar fluids to fit the f_{int} factor in the Eucken correlation. Data at high densities are used to fit a new thermal conductivity shape factor χ. With such data, the method yields deviations which are

often comparable with the scatter in the data and the systematic differences between various data sources. The method reproduces experimental thermal conductivities with average absolute deviations of less than 4% for 12 of the 14 fluids studied. The critical enhancement is treated empirically in the method, and further work on this contribution to the thermal conductivity is needed.

For mixtures, the average absolute deviations are less than 6% for nine of the 12 mixtures studied. These results are purely predictive in that no additional mixture-specific parameter is employed. Both the dilute-gas contribution and the critical enhancement for mixtures are treated empirically in the method. The systematic deviations seen with most of the mixtures suggest the need for some sort of adjustable mixture parameter. The present state of theory indicates that an empirical mixture parameter is likely to be the more fruitful avenue of investigation. Comparisons to data show that the present approach gives reasonable results which should suffice for most engineering purposes.

Acknowledgements

We thank M. Huber and E. Lemmon for providing their files of literature data for many of the fluids. We thank D. Friend and M. Huber for many helpful discussions. This work has been supported by the US Department of Energy, Office of Building Technology (grant number DE-FG02-91CE23810: Materials Compatibilities and Lubricants Research on CFC-Refrigerant Substitutes) through the Air-Conditioning and Refrigeration Technology Institute. This support does not constitute an endorsement by the US DoE, or by the air-conditioning and refrigeration industry, of the views expressed herein. The stay of S.A.K. at NIST was funded, in part, by the University of Wisconsin and by a grant from the National Science Foundation under Agreement no. 9527385. Any opinions, findings, and conclusions or recommendations expressed in this publication are those of the authors and do not necessarily reflect the views of the National Science Foundation.

Appendix

The thermal conductivity of the R134a reference fluid is represented by the correlation of Perkins et al. [12]. Since this reference may not be readily available to some readers, we repeat this correlation to fully document the ECS model presented here. The thermal conductivity is the sum of three terms:

$$\lambda(T,\rho) = \lambda^{\mathrm{d.g.}}(T) + \lambda^{\mathrm{r}}(T,\rho) + \lambda^{\mathrm{crit}}(T,\rho). \tag{A1}$$

The dilute-gas contribution is the sum of λ^{int} and λ^{*} in Eq. (1). It is an empirical function of temperature:

$$\lambda^{\mathrm{d.g}} = a_0 + a_1 T. \tag{A2}$$

(The values of the parameters in the equations in this appendix are given in Table A1.) The residual contribution is an empirical polynomial in reduced density:

Table A1
Parameters in the R134a reference fluid formulation of Perkins et al. [12]

Tableau A1
Paramètres de la formulation de références R134a de Perkins et al. [12]

Parameter	Value	Units	Interpretation
a_0	-1.05248×10^{-2}	W m^{-1} K^{-1}	Empirical parameter
a_1	8.00982	W m^{-1} K^{-2}	Empirical parameter
b_1	1.836526	–	Empirical parameter
b_2	5.126143	–	Empirical parameter
b_3	−1.436883	–	Empirical parameter
b_4	0.626144	–	Empirical parameter
$\lambda^{\mathrm{reducing}}$	2.055×10^{-3}	W m^{-1} K^{-1}	Reducing factor
q_{D}	1.89202×10^{9}	m^{-1}	Modified effective cutoff wave number
ξ_0	1.94×10^{-10}	m	Critical amplitude
Γ	0.0496	–	Amplitude
T_{ref}	561.411	K	Arbitrary reference temperature
P^{crit}	4059.28	kPa	Critical pressure
ρ^{crit}	5.017053	mol L^{-1}	Critical density
ν	0.63	–	Universal exponent
γ	1.239	–	Universal exponent
R_0	0.63	–	Universal amplitude

$$\lambda^{r}/\lambda^{\text{reducing}} = b_1\left(\frac{\rho}{\rho^{\text{crit}}}\right) + b_2\left(\frac{\rho}{\rho^{\text{crit}}}\right)^2 + b_3\left(\frac{\rho}{\rho^{\text{crit}}}\right)^3 + b_4\left(\frac{\rho}{\rho^{\text{crit}}}\right)^4,$$

where $\lambda^{\text{reducing}}$ is a reducing is a reducing factor used to convert units.

The critical enhancement for thermal conductivity uses the "simplified" model presented by Vesovic et al. [62]:

$$\lambda^{\text{crit}} = \rho C_P \frac{R_0 kT}{6\pi\varepsilon\xi}(\tilde{\Omega} - \tilde{\Omega}_0), \tag{A4}$$

where the isobaric heat capacity C_P is from the equation of state of Tillner-Roth and Baehr [14], and the viscosity η is computed using the correlation of Laesecke, which was presented in our earlier paper on viscosity [2]. R_0 is a "universal amplitude," and k is Boltzmann's constant. The correlation length ξ is

$$\xi = \xi_0\left[\frac{1}{\Gamma}(\chi^*(T,\rho) - \chi^*(T_{\text{ref}},\rho))\right]^{(\nu/\gamma)}, \tag{A5}$$

where the dimensionless susceptibility

$$\chi^*(T,\rho) = \frac{\rho P^{\text{crit}}}{(\rho^{\text{crit}})^2}\left(\frac{\partial\rho}{\partial P}\right)_T \tag{A6}$$

is evaluated at the temperature and density of interest and at an arbitrary reference temperature T_{ref}, here set to 1.5 times the critical temperature. The crossover functions Ω and Ω_0 are given by

$$\Omega = \frac{2}{\pi}\left[\left(\frac{C_p - C_v}{C_p}\right)\tan^{-1}(q_D\zeta) + \frac{C_v}{C_p}q_D\zeta\right] \tag{A7}$$

and

$$\Omega_0 = \frac{2}{\pi}\left\{1 - \exp\left[\frac{-1}{(q_D\zeta)^{-1} + \frac{1}{3}(q_D\zeta\rho^{\text{crit}}/\rho)^2}\right]\right\}. \tag{A8}$$

In this model for the critical enhancement, the "modified effective cutoff wave number" q_D and the critical amplitudes ξ_0 and Γ are the only fluid-specific parameters. The remaining parameters are universal (although different interpretations sometimes result in slightly different numerical values) and are given in Table A1.

References

[1] Huber ML, Friend DG, Ely JF. Prediction of the thermal conductivity of refrigerants and refrigerant mixtures. Fluid Phase Equilibria 1992;80:249–61.

[2] Klein SA, McLinden MO, Laesecke A. An improved extended corresponding states method for estimation of viscosity of pure refrigerants and mixtures. Int J Refrigeration 1997;20:208–17.

[3] Ely JF, Hanley HJM. Prediction of transport properties. 2. Thermal conductivity of pure fluids and fluid mixtures. Ind Eng Chem, Fund 1983;22:90–7.

[4] Hirschfelder JO, Curtiss CF, Bird RB. Molecular theory of gases and liquids. New York: John Wiley and Sons, Inc, 1967.

[5] Reid RC, Prausnitz JM, Poling BE. The properties of gases and liquids. 4th ed. New York: McGraw–Hill, 1987.

[6] Neufeld PD, Janzen AR, Aziz RA. Empirical equations to calculate 16 of the transport collision integrals $\Omega^{(l,s)*}$ for the Lennard–Jones (12–6) potential. J Chem Phys 1972;57:1100–2.

[7] Huber ML, Ely JF. Prediction of the viscosity of refrigerants and refrigerant mixtures. Fluid Phase Equilibria 1992;80:239–48.

[8] Leland TW, Chappelear PS. The corresponding states principle. AIChE J 1968;14:568–76.

[9] Hanley HJM. Prediction of the viscosity and thermal conductivity coefficients of mixtures. Cryogenics 1976;16(11):643–51.

[10] Ely JF, Hanley HJM. Prediction of transport properties. 1. Viscosity of fluids and mixtures. Ind Eng Chem, Fund 1981;20:323–32.

[11] Press WH, Flannery BP, Teukolsky SA, Vettering WT. Numerical recipes: the art of scientific computing. Cambridge: Cambridge University Press, 1986.

[12] Perkins RA, Laesecke A, Howley JB, Huber ML, Nieto de Castro CA. Experimental thermal conductivity and thermal diffusivity values for R32, R125, and R134a. National Institute of Standards and Technology, NISTIR, in preparation.

[13] Assael MJ, Nagasaka Y, Nieto de Castro CA, Perkins RA, Ström K, Vogel E, Wakeham WA. Status of the round robin on the transport properties of R134a. Int J Thermophysics 1995;16(1):63–78.

[14] Tillner-Roth R, Baehr HD. An international standard formulation of the thermodynamic properties of 1,1,1,2-tetrafluoroethane (HFC-134a) covering temperatures from 170 K to 455 K at pressures up to 70 MPa. J Phys Chem Ref Data 1994;23:657–729.

[15] Donaldson AB. On the estimation of thermal conductivity of organic vapors. Ind Eng Chem 1975;14:325–8.

[16] Geller VZ, Artamonov SD, Zaporozhan GV, Peredrii VG. Thermal conductivity of Freon-12. J Eng Phys 1974;27:842–6.

[17] Keyes FG. Thermal conductivity of gases. Trans ASME 1954;76:809–16.

[18] Makita T, Tanaka Y, Morimoto Y, Noguchi M, Kubota H. Thermal conductivity of gaseous fluorocarbon refrigerants R12, R13, R22, and R23 under pressure. Int J Thermophysics 1981;2:249–68.

[19] Shankland IR. Transport properties of CFC alternatives. Paper presented at AIChE Spring National Meeting, Orlando, FL, 1990.

[20] Sherratt GG, Griffiths E. A hot wire method for the thermal conductivity of gases. Phil Mag 1939;27:68–75.

[21] Venart JES, Mani N. The thermal conductivity of R12. Trans Canadian Soc Mech Engrs 1975;3:1–9.
[22] Yata J, Minamiyama T, Tanaka S. Measurement of thermal conductivity of liquid fluorocarbons. Int J Thermophysics 1984;5:209–18.
[23] Grebenkov AJ, Kotelevsky YG, Saplitza VV, Beljaeva OV, Zajatz TA, Timofeev BD. Experimental study of thermal conductivity of some ozone safe refrigerants and speed of sound in their liquid phase. CFCs: The Day After, Joint Meeting of IIR Commissions B1, B2, E1, and E2, Padova, Italy, 21–23 September, 1994, IIR, 419–429.
[24] Tsvetkov OB, Laptev YA, Asambaev AG. Thermal conductivity of refrigerants R123, R134a and R125 at low temperatures. Int J Thermophysics 1993;15:203–14.
[25] Wilson LC, Wilding WV, Wilson GM, Rowley RL, Felix VM, Chilsom-Carter T. Thermophysical properties of HFC-125. Fluid Phase Equilibria 1992;80:167–77.
[26] Clifford AA, Tufeu R. Thermal conductivity of gaseous and liquid ammonia. Journal of Heat Transfer 1988;110:992–5.
[27] Frank EU. Zur Temperaturabhängigkeit der Wärmëleitfähigkeit einiger Gase. Z Elektrochemie 1951;55:636–43.
[28] Golubev IF, Sokolova VP. The thermal conductivity of ammonia at various temperatures and pressures. Thermal Engineering 1994;11:78–82.
[29] Needham DP, Ziebland H. The thermal conductivity of liquid and gaseous ammonia and its anomalous behaviour in the vicinity of the critical point. International Journal of Heat and Mass Transfer 1965;8:1387–414.
[30] Richter GN, Sage BH. Thermal conductivity of fluids: ammonia. J Chem Eng Data 1964;9:75–8.
[31] Tufeu R, Ivanov DY, Garrabos Y, Le Neindre B. Thermal conductivity of ammonia in a large temperature and pressure range including the critical region. Ber Bunsen-Ges Phys Chem 1984;88:422–7.
[32] Tillner-Roth R, Harms-Watzenberg F, Baehr HD. Eine neue Fundamentalgleichung für Ammoniak. DKV-Tagungsbericht 1993;20(II):167–81.
[33] Ely JF, Magee JW, Haynes WM. Thermophysical properties for special high CO_2 content mixtures. Research Report RR-110, Gas Processors Association, Tulsa, OK, 1987.
[34] Johns AI, Rashid S, Watson JTR, Clifford A. Thermal conductivity of argon, nitrogen and carbon dioxide at elevated temperatures and pressures. J Chem Soc Faraday Trans I 1986;82:2235–46.
[35] Johnston HL, Grilly ER. The thermal conductivities of eight common gases between 80° and 380°K. J Chem Phys 1946;14:233–8.
[36] Millat J, Mustafa M, Ross M, Wakeham WA, Zalaf M. The thermal conductivity of argon, carbon dioxide and nitrous oxide. Physica A 1987;145:461–97.
[37] Scott AC, Johns AI, Watson JTR, Clifford AA. Thermal conductivity of carbon dioxide in the temperature range 300–348 K and pressures up to 25 MPa. J Chem Soc Faraday Trans I 1983;79:733–40.
[38] Younglove BA, Ely JF. Thermophysical properties of fluids. II. Methane, ethane, propane, isobutane and normal butane. J Phys Chem Ref Data 1987;16:577–798.
[39] Aggarwal MC, Springer GS. High temperature-high pressure thermal conductivities of ethylene and propane. J Chem Phys 1979;70:3948–51.
[40] Mann WB, Dickins BG. The thermal conductivities of the saturated hydrocarbons in the gaseous state. Proc Royal Soc (London), Series A 1932;134:77–96.
[41] Roder HM. Experimental thermal conductivity values for hydrogen, methane, ethane and propane. National Bureau of Standards NBSIR 84–3006, 1984.
[42] Tufeu R, LeNeindre B. Thermal conductivity of propane in the temperature range 25–305°C and pressure range 1–70 MPa. Int J Thermophysics 1987;8:27–38.
[43] Jacobsen RT, Penoncello SG, Lemmon EW. A fundamental equation for trichlorofluoromethane (R-11). Fluid Phase Equilibria 1992;80:45–56.
[44] Richard RG, Shankland IR. A transient hot-wire method for measuring the thermal conductivity of gases and liquids. Int J Thermophysics 1989;10:673–86.
[45] Marx V, Pruß A, Wagner W. Neue Zustandsgleichungen für R12, R22, R11 und R113. Beschreibung des thermodynamishchen Zustandsverhaltens bei Temperaturen bis 525 K und Drücken bis 200 MPa, VDI-Fortschritt-Ber. Series 19, No. 57, Düsseldorf: VDI Verlag, 1992
[46] Platzer B, Maurer G. A generalized equation of state for pure polar and nonpolar fluids. Fluid Phase Equilib 1989;51:223–36.
[47] Geller V, Peredrii VG. Thermal conductivity of Freon 13 and Freon 2. Izv Vyssh Uchebn Zaved Energetika 1975;18:113–6(in Russian).
[48] Kamei A, Beyerlein SW, Jacobsen RT. Application of nonlinear regression in the development of a wide range formulation for HCFC-22. Int J Thermophysics 1995;16(5):1155–64.
[49] Assael MJ, Karagiannidis E. Measurements of the thermal conductivity of R22, R123, and R134a in the temperature range 250–340 K at pressures up to 30 MPa. Int J Thermophysics 1993;14:183–97.
[50] Tsvetkov OB, Laptev YA. Thermal conductivity of difluoromonochloromethane in the critical region. Int J Thermophysics 1991;12:53–65.
[51] McLinden MO, Klein SA, Lemmon EW, Peskin AP. NIST Standard Reference Database 23, NIST thermodynamic and transport properties of refrigerants and refrigerant mixtures—REFPROP, version 6.0. Standard Reference Data Program, National Institute of Standards and Technology, 1998.
[52] Tillner-Roth R, Yokozeki A. An international standard equation of state for difluoromethane (R-32) for temperatures from the triple point at 136.34 K to 435 K and pressures up to 70 MPa. J Phys Chem Ref Data 1997;26:1273–328.
[53] Hahne E, Gross U, Song YW. The thermal conductivity of R115 in the critical region. Int J Thermophysics 1989;10:687–700.
[54] Outcalt SL, McLinden MO. Equations of state for the thermodynamic properties of R32 (difluoromethane) and R125 (pentafluoroethane). Int J Thermophysics 1995;16:79–89.
[55] Perkins RA, Laesecke A, Nieto de Castro CA. Polarized transient hot wire thermal conductivity measurements. Fluid Phase Equilibria 1992;80:275–86.
[56] Sousa AT, Fialho PS, Nieto de Castro CA, Tufeu R, LeNeindre B. The thermal conductivity of 1-chloro-1,1-difluoroethane. Int J Thermophysics 1992;13:383–99.

[57] Tanaka Y, Nakata M, Makita T. Thermal conductivity of gaseous HFC-134a, HFC-143a, HCFC-141b, and HCFC-142b. Int J Thermophysics 1991;12:949–63.
[58] Yata J, Hori M, Kobayashi K, Minamiyama T. Thermal conductivity of alternative fluorocarbons in the liquid phase. Int J Thermophysics 1996;17:561–71.
[59] Outcalt SL, McLinden MO. An equation of state for the thermodynamic properties of R143a (1,1,1-trifluoroethane). Int J Thermophysics 1997;18:1445–63.
[60] Haynes WM. Thermophysical properties of HFC-143a and HFC-152a. Final Report for ARTI MCLR Project Number 660-50800. National Institute of Standards and Technology, Boulder, CO, 1994.
[61] Fenghour A, Wakeham WA, Vesovic V, Watson JTR, Millat J, Vogel E. The viscosity of ammonia. J Phys Chem Ref Data 1995;24:1649–67.
[62] Vesovic V, Wakeham WA, Olchowy GA, Sengers JV, Watson JTR, Millat J. The transport properties of carbon dioxide. J Phys Chem Ref Data 1990;19:763–808.
[63] Vogel E, Kuchenmeister C, Bich E, Laesecke A. Reference correlation of the viscosity of propane. J Phys Chem Ref Data 1998;27:947–70.
[64] Takahashi M, Takahashi S, Iwasaki H. Viscosity of gaseous chlorodifluoromethane (R-22). Kagaku Kogaku Ronb 1983;9:482–4.
[65] Takahashi M, Shibasaki-Kitakawa N, Yokoyama C, Takahashi S. Gas viscosity of difluoromethane from 298.15 K to 423.15 K and up to 10 MPa. J Chem Eng Data 1995;40:900–2.
[66] Assael MJ, Papadopoulos AA, Polimatidou S. Measurements of the viscosity of refrigerants in the vapour phase. 4th Asian Thermophysical Properties Conference, Tokyo 1995;3:623–6.
[67] Mason EA, Uribe FJ. The corresponding-states principle: dilute gases. In: Transport properties of fluids. Cambridge: Cambridge University Press, 1996. p. 250–282.
[68] Perkins RA, Schwarzberg E, Gao X. Experimental thermal conductivity and thermal diffusivity values for mixtures of R32, R125, R134a, and propane. National Institute of Standards and Technology, NISTIR, in preparation.
[69] Perkins RA, Private communication, National Institute of Standards and Technology, Boulder, CO, 1999.
[70] Mason EA, Saxena SC. Approximate formula for the thermal conductivity of gas mixtures. Phys Fluids 1958;1:361–9.
[71] Wassiljewa A. Wörmeleitung in Gasgemischen. Phys Z 1904;5:737–42.
[72] Ely JF, Hanley HJM. A computer program for the prediction of viscosity and thermal conductivity of hydrocarbon mixtures. National Bureau of Standards, NBS Technical Note 1039, 1981.
[73] Huber ML, Hanley HJM. The corresponding-states principle: dense fluids. In: Transport properties of fluids, Cambridge: Cambridge University Press, 1996, p. 283–9.
[74] Huber ML, Hanley HJM. Private communication. National Institute of Standards and Technology, Boulder, CO, 1999.
[75] Friend DG, Ely JF. Thermodynamic properties of the methane–ethane system. Fluid Phase Equilibria 1992;79:77–88.
[76] Lemmon EW. A generalized model for the prediction of the thermodynamic properties of mixtures including vapor–liquid equilibrium. Ph.D. dissertation, University of Idaho, Moscow, ID, 1996.
[77] Lemmon EW, Jacobsen RT. Thermodynamic properties of mixtures of R-32, R-125, R-134a, and R-152a. Int. J. Thermophysics, in press.
[78] Kiselev SB, Huber ML. Transport properties of carbon dioxide + ethane and methane + ethane mixtures in the extended critical region. Fluid Phase Equilibria 1998;142:253–80.